Chapter 2

Sizes and albedos of asteroids: the radiometric method and asteroid thermal models

2.1 Foreword

Even on the largest 10m class telescopes most NEAs appear as point like sources. However, the *size* and the *albedo* of an atmosphere-less body can be derived by means of the so-called radiometric technique, which combines observations obtained in the thermal infrared region with the visible brightness of the object. In this chapter we illustrate the basis of this method which makes use of thermal models describing how the infrared radiation is emitted from the surface of the body. We introduce the Standard Thermal Model (STM), the Fast Rotating Thermal Model (FRM) and the NEATM, the near Earth asteroid thermal model and we give details of the algorithms used for their implementation. Assumptions involved in the use of thermal models cause the resulting asteroid diameters and albedos to be model dependent and affected by uncertainties which are discussed in section 2.8. Flux variability due to asteroid rotation alters the shape and the mean intensity of the measured spectral energy distribution. We introduce a method to refer measured infrared fluxes to lightcurve mean magnitude when visible lightcurve data are available for the epoch of thermal infrared measurements. The latter correction, which can be neglected for large main-belt asteroids, is proven to be of crucial importance for small and irregular bodies often observed at large phase angles, as NEAs are.

2.2 Introduction

With modern medium infrared instrumentation, equipping the largest existing telescopes, it is possible to measure the weak thermal infrared emission of NEOs, down to sizes of the order of some hundred meters.

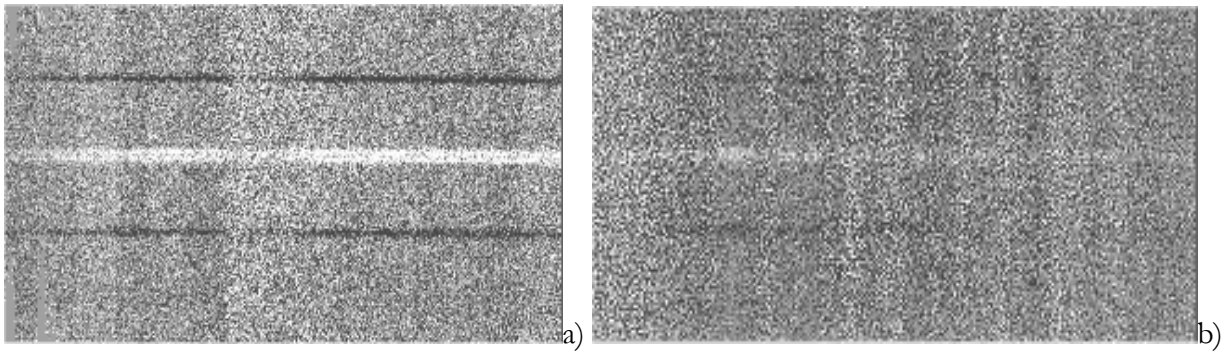

Fig. 2.1 N-band a) and Q-band b) spectra of the thermal infrared emission of the near-earth asteroid 5587 (1990SB) observed on April 09, 2001 with the TIMMI2 installed at the 3.6m telescope, La Silla, ESO (Chile). This asteroid has a diameter of almost 4km.

By comparison with calibration stars, the spectral energy distribution of which is known to high accuracy (i.e. 3%, see Cohen et al, 1999), asteroids raw data are converted to infrared fluxes. Chapter 3 of this work is manly devoted to the methods of thermal infrared photometry that we have developed to derive asteroid infrared fluxes from observations obtained at Keck, ESO, NASA-IRTF telescopes. Fig. 2.2 shows examples for thermal infrared spectra of asteroids.

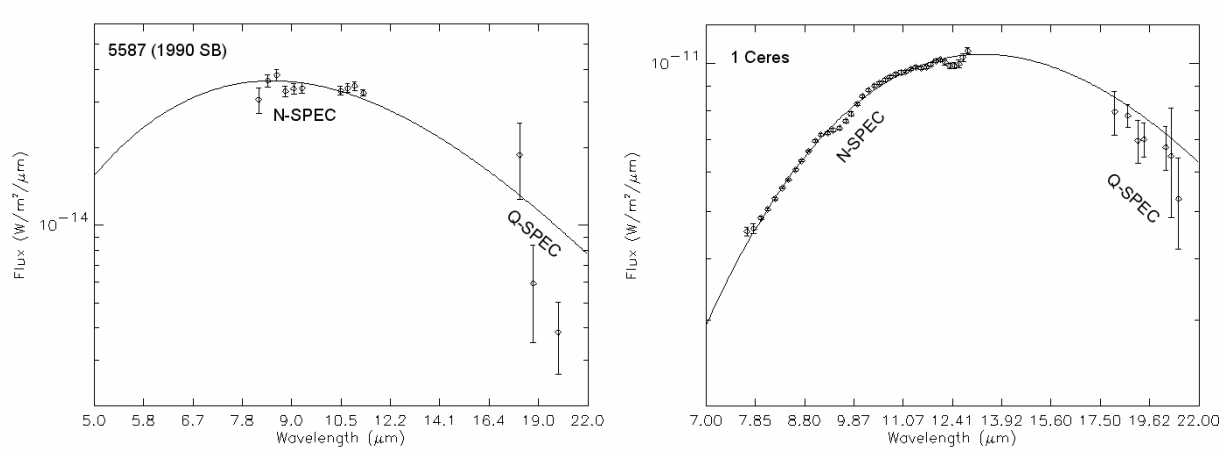

Fig. 2.2 Observed thermal infrared fluxes of the NEA 5587 on the left and of the largest asteroid 1 Ceres. Note the noise affecting Q-band data which have been binned for increasing the signal to noise ratio. Continuous line is a black body fit to the infrared spectra.

In contrast to reflected visible light, thermal infrared radiation carries direct information about the size of the asteroid: to first-order approximation, one can describe the observed thermal energy distribution (Fig. 2.2) as the emission of a black body at an effective temperature T_{eff} multiplied by the material emissivity $\varepsilon(\lambda)$ and by the solid angle the radiator subtends on the sky i.e.

$$F(\lambda) = \frac{A_p}{\Delta^2}\varepsilon(\lambda)B(\lambda, T_{eff}) \qquad (2\text{-}1)$$

where B(λ,T) is the Planck radiation function

$$B(\lambda, T) = \frac{2\pi hc^2\lambda^{-5}}{e^{hc/\lambda KT} - 1} \qquad (2\text{-}2)$$

The term A_p of Eq. (2-1) is the emitting area of the thermal radiator projected along the line-of-sight. The distance of the object from the observer, Δ, is known from the ephemerides of the asteroid. If we assume the emissivity to be constant and known at every wavelength (it is common practice to assume that asteroid surfaces have $\varepsilon(\lambda)=0.9$ for wavelengths in the range 5-20 μm), in Eq. (2-1) we have only two unknowns: A_p and T_{eff}. If the spectral energy distribution of the thermal radiator has been sampled

at several infrared wavelengths λ_i, i=[1...N], Eq. (2-1) can be evaluated at those λ_i and we can, finally, write a system of non-linear equations: one equation for each measured spectral data point:

$$\begin{cases} F(\lambda_1) = \dfrac{A_p}{\Delta^2}\varepsilon(\lambda)B(\lambda_1, T_{eff}) \\ \quad .... \\ F(\lambda_N) = \dfrac{A_p}{\Delta^2}\varepsilon(\lambda)B(\lambda_N, T_{eff}) \end{cases} \tag{2-3}$$

A solution to system (2-3) can be found by a non-linear least square fit. A very effective method to be used in such cases is the *Levenberg-Marquardt* algorithm described, for instance, by Press et al. (2002), section 15.5. Such method allows the projected area and thus the effective diameter of an asteroid to be retrieved with typical accuracy of about 10%. The effective surface temperature is derived simultaneously with errors of no more than 10-20 K. At low solar phase angles, the assumption that the emitting projected area of the thermal radiator corresponds to the actual area of the object projected on the sky introduces an error of negligible contribution, given the other source of uncertainties, such as the absolute calibration of the infrared flux. We thus can obtain the unknown size of the asteroid in this very simple way. Unfortunately, for very weak targets it is not always possible to obtain measurements of the spectral energy distribution to a level of accuracy good enough to allow a stable solution to Eq. 2-1 to be found. In those cases, we have to rely on different methods which make use of models (thermal models) describing how the thermal infrared emission at the surface of asteroids originates. The first step in modeling the thermal emission of asteroids is to estimate the surface temperature distribution.

2.3 Asteroid surface temperatures

The temperature of a surface element of an asteroid is a function of the distance from the Sun, albedo, emissivity, and angle of inclination to the solar direction. A dark object absorbs more solar radiation than what brighter one does, which results in a higher equilibrium temperature. The total incoming energy incident on a surface element of area dS is:

$$dU_i = \frac{S_0}{r^2}\mu dS \tag{2-4}$$

where μ is the direction cosine of the normal to the surface with respect to the solar direction, S_0 the solar constant and r the heliocentric distance of the asteroid. Energy that is not reflected is absorbed by the asteroid surface:

$$dU_a = dU_i(1 - A) \tag{2-5}$$

where A is the bolometric Bond albedo, which is the ratio of total scattered solar energy in all directions and at all wavelengths to the incident energy. The absorbed energy and has to be balanced by thermal emission. The energy emitted by a surface dS with emissivity ε at a temperature T is:

$$dU_e = \sigma \varepsilon T^4 dS \tag{2-6}$$

where σ is the Stefan–Boltzmann's constant. Assuming that each element of the surface is in instantaneous equilibrium with solar radiation, conservation of energy implies that $dU_a = dU_e$. The following equation for a surface element at the subsolar point ($\mu = 1$) can be written:

$$\frac{S_0(1-A)}{r^2} dS = \sigma \varepsilon T_{SS}^4 dS \Rightarrow \frac{S_0(1-A)}{r^2} = \sigma \varepsilon T_{SS}^4 \tag{2-7}$$

Eq (2-7) can be used to derive the value of T_{SS}, the maximum (sub-solar) temperature, as a function of heliocentric distance, r, and Bond albedo, A via the relation:

$$T_{SS} = \left[\frac{S_0(1-A)}{\sigma \varepsilon \, r^2} \right]^{\frac{1}{4}} \tag{2-8}$$

Fig. 2.3 shows the dependence of T_{SS} as a function of the heliocentric distance and Fig. 2.4 shows the dependence of the sub-solar temperature of an asteroid as a function of the bolometric Bond albedo A. A is proportional to the geometric visible albedo p_V via the relation:

$$A \cong A_V = q \times p_V \tag{2-9}$$

where q is the phase integral which allows the parameter A to be linked directly to p_V. The geometric visual albedo p_V, which is defined as the ratio of the visual brightness of a planetary body observed at zero phase angle to that of a perfectly diffusing "Lambertian" disk of the same radius and at the same distance as the body, is a measurable and widely quoted parameter. In the standard H, G magnitude system described by Bowell et al. (1989), in which H is the absolute magnitude and G is the slope parameter we have that:

$$q = 0.290 + 0.684 \times G \tag{2-10}$$

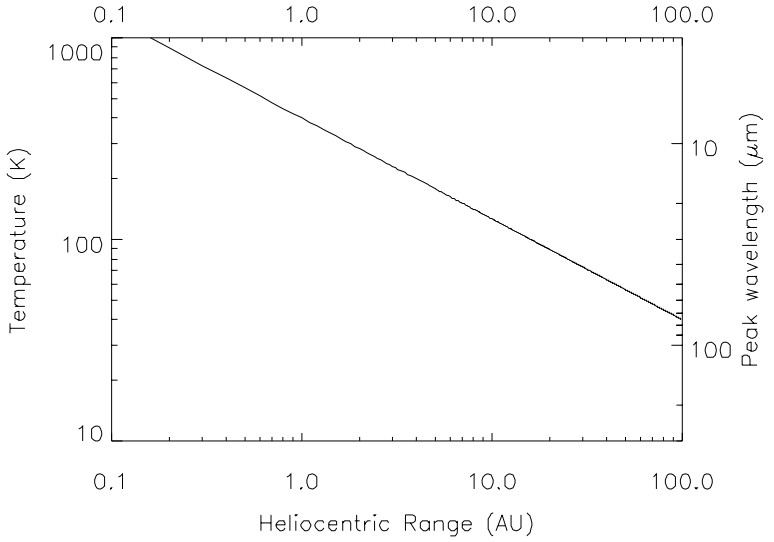

Fig. 2.3 Dependence of the sub-solar temperature as a function of its heliocentric distance for an asteroid in instantaneous thermal equilibrium with sunlight at all points on its surface. For objects orbiting the Sun in the near-Earth space, the surface temperature is about 400K and the emitted thermal radiation peaks around 8 μm. However, the radiation of more distant asteroids shifts toward longer wavelength as their temperature decreases. The following parameters have been used to produce the plot: A = 0.0393 (corresponding to p_V = 0.1 and G = 0.15) emissivity = 0.9, and solar constant = 1373 W m^{-2}.

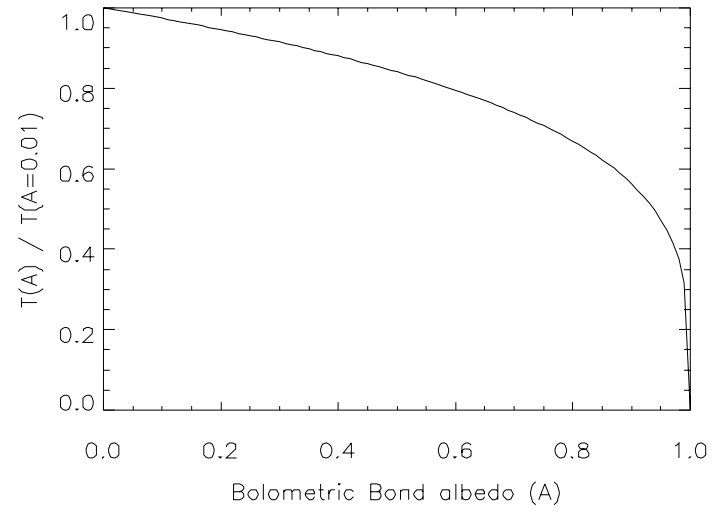

Fig. 2.4 Dependence of the sub-solar temperature of an asteroid as a function of the bolometric Bond albedo A. This dependence does not depend on the heliocentric distance of the body.

The equation of thermal equilibrium can be used not only to estimate the maximum temperature, but it determines the distribution of temperatures on the surface as well:

$$\frac{S_0(1-A)}{r^2}\mu = \sigma\varepsilon T^4(\mu) \tag{2-11}$$

and in the case of a sphere, where the direction cosine is a simple function of the solar colatitude Ω (μ=cos Ω)

$$\frac{S_0(1-A)}{r^2}\cos\Omega = \sigma\varepsilon T^4(\Omega) \Rightarrow \begin{cases} T(\Omega) = T_{SS}(\cos\Omega)^{\frac{1}{4}} & \text{for } \Omega \le \pi/2 \\ T(\Omega) = 0 & \text{otherwise} \end{cases} \tag{2-12}$$

Eqs. 2-8 and 2-12 are very important: they define the temperature distribution of a sphere on the assumption of instantaneous thermal equilibrium with sunlight at all points on its surface (Equilibrium Model, hereafter EM).

2.4 Calculation of the emitted thermal infrared flux

Once the temperature distribution is known (or it has been assumed), to calculate the emitted infrared flux received by an observer at a distance Δ from the asteroid is easily achieved by numerically integrating the contribution of each surface element visible to the observer, i.e.:

$$F(\lambda) = \frac{\varepsilon(\lambda)}{\Delta^2}\iint_{\Pi} B(\lambda,T)d\Omega \tag{2-13}$$

where dΩ is the projected area of the surface element, Π is the asteroid projected surface and B(λ,T) is the Planck radiation formula. The model infrared flux scales with the projected area (i.e. with the square of the effective diameter). So, if we evaluate the integral of Eq. (2-13) on a "reference" asteroid with a emitting projected area equal to $\pi/4$ km^2 (i.e. an asteroid with effective diameter of 1 km)

$$F_{reference}(\lambda) = \frac{\varepsilon(\lambda)}{\Delta^2}\iint_{\Pi_{reference}} B(\lambda,T)d\Omega\,, \tag{2-14}$$

we obtain a direct relationship between the asteroid effective diameter and the measured infrared flux:

$$D_{eff}^2 = F_{measured}(\lambda)/F_{reference}(\lambda)\,. \tag{2-15}$$

Since $F_{reference}(\lambda)$ is a function of p_V, the ratio of Eq 2-15 is a function of the geometric visible albedo too. The trajectory of this function is shown in Fig. 2.5

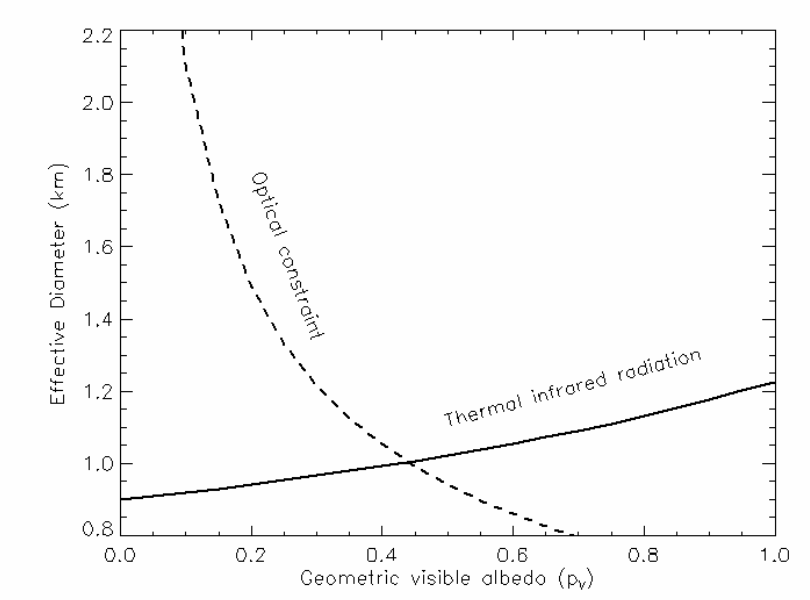

Fig. 2.5 Constraints on the albedo and effective diameter from thermal infrared observations and visible absolute magnitude. Solid line: curve defined by Eq. (2-15), dashed-line: curve defined by Eq. (2-16).

2.5 Constraints on diameter and albedo from the visible absolute magnitude

The absolute magnitude H of an asteroid, which correspond to the magnitude in the V-band measured (or extrapolated) at zero degree of phase angle, at the heliocentric and geocentric distance of 1AU is related to the geometric visible albedo, p_V, and the asteroid effective diameter D_{eff} by the relation (e.g. Fowler and Chillemi, 1986):

$$D_{eff} = \frac{1329}{\sqrt{p_V}} 10^{-\frac{H}{5}} \qquad (2\text{-}16)$$

Given the H value, this equation defines the second curve shown in Fig. 2.5 by plotting the diameter as a function of the albedo. The intersection of the two curves gives the best estimate for the diameter and the albedo of the asteroid.

2.6 Radiometric diameters and albedos

The method described above defines the basis for the radiometric determination of asteroid sizes and albedos. The principle of this technique has been outlined by Morrison (1973). Furthermore, it is of interest to see Lebofsky and Spencer (1989) and Tedesco (1992). Delbo & Harris (2002) and Harris and Lagerros (2002) provided recent review of the principle on which this technique is based.

2.7 Thermal models of asteroids

As already described, several assumptions have to be made to determine the bolometric albedo from the visual albedo and a model is required to describe the temperature distribution on the surface of the asteroid and the way infrared radiation is emitted from a body of given size and bolometric albedo.

In section 2.5 we have discussed a method to derive diameters and albedos of atmosphere-less bodies of the Solar System, which assumes a non-rotating spherical shape in thermal equilibrium with solar radiation. Furthermore, the method works at zero degrees of solar phase angle only. However, real asteroids are not spherical, neither they are observed at $\alpha=0°$. Moreover, in the case of objects with known size, it was observed that the assumption of thermal equilibrium leads to a zero-phase-angle model infrared flux which is too small compared to observations. Resulting asteroids diameters derived on the assumption of thermal equilibrium are thus larger than what they actually are. Modifications to the simple equilibrium model were therefore introduced to account for asteroid rotation, to compensate for the angular distribution of the thermal emission, to adjust the surface temperature to match the observed color temperature etc.

In the next sessions, we introduce the three different asteroid thermal models that will be fitted to the measured infrared fluxes to calculate diameters and albedos.

2.7.1 The Standard Thermal Model (STM)

The vast majority of asteroid diameters and albedos, including those in the IRAS minor planet survey (Tedesco, 1992), and those in the new release of the Supplemental IRAS Minor Planet Survey – SIMPS – (Tedesco et al., 2002) have been derived using the Standard Thermal Model (STM). The basis of the STM is the assumption of a spherical shape and instantaneous equilibrium between insolation and thermal emission at each point on the surface. It was designed to work at zero degree of solar phase angle. The angular dependence of the temperature distribution is described by Eq. 2-11. The temperature falls to zero at the terminator and there is no thermal emission from the night side. However, the "refined" STM of Lebofsky et al. (1986) and Lebofsky and Spencer (1989) includes a modification to the sub-solar temperature T_{SS} via the so-called beaming parameter η. The η parameter was introduced to match the occultation diameter of large main belt asteroids and it was included to account for the enhancement in the thermal radiation observed at small phase angles. This tendency of the radiation to be "beamed" towards the Sun is similar to the opposition effect (see Belskaya and Shevchenko, 2000) in the visible light. In the refined STM of Lebofsky and Spencer its value is set to 0.756 to match the occultation diameter of 1 Ceres and 2 Pallas. One more point has to be addressed:

observations are almost never carried out at zero degree of solar phase angle. Matson (1971) and Lebosfky and Spencer (1986) observed that asteroids had infrared phase curves which could be approximated by a linear function up to phase angles of about 30°. They derived a mean phase coefficient β_E of 0.01 magnitudes/degree. The STM should give accurate results for an asteroid that has thermal properties similar to those of large main-belt asteroids and is observed at a small phase angle. STM was designed to work with asteroid infrared magnitudes measured at a single wavelength. In those cases where infrared data were available at different wavelengths radiometric resulting diameters and albedos were given for each wavelength. It is common practice, for example, to speak of 10-μm or 20-μm diameters of asteroids. However, if photometric data are available at more than one wavelength the STM can be applied to all data points simultaneously searching for a least-square solution by minimizing the χ^2 of the residuals observed fluxes – predicted model fluxes. In this work, the STM is implemented by means of the following algorithm:

1. Guess the geometric visible albedo p_V.
2. Given the H value, calculate D from Eq. 2-16
3. From Eq. 2-8, obtain A and calculate T_{SS} using Eq (2-17) with η=0.756

$$T_{SS} = \left[\frac{S_0}{r^2} \frac{(1-A)}{\eta \varepsilon \sigma} \right]^{1/4} \tag{2-17}$$

4. Calculate the temperature distribution on the surface of the sphere

$$T(\Omega) = T_{SS} \cos^{1/4} \Omega \tag{2-18}$$

where Ω is the angular distance from the sub-solar point (i.e. the colatitude in a reference frame with the pole pointing towards the Sun).

5. Calculate the model flux

$$F(\lambda_i) = \frac{\varepsilon D^2}{2\Delta^2} \int_0^{\pi/2} B(\lambda_i, T(\Omega)) \cos\Omega \sin\Omega d\Omega \tag{2-19}$$

6. Scale the observed flux to zero degree of phase angle, α

$$f(\lambda_i) = f_{observed}(\lambda_i) \times 10^{-(0.01 \times |\alpha|)/2.5} \tag{2-20}$$

7. Calculate the χ^2

$$\chi^2 = \sum_{i=1}^{N} \left(\frac{(F(\lambda_i) - f(\lambda_i))^2}{\sigma_i^2} \right) \tag{2-21}$$

8. Change the value of the p_V parameter and reiterate the algorithm (going back to point 2) until the minimum value of the χ^2 is reached.

The value of the p_V at χ^2 minimum is the least-square best estimate for the albedo of the asteroid. The diameter D is simultaneously set to its best (least-square) estimate by Eq (2-16).

2.7.2 The Fast Rotating Model (FRM)

Problems arise in the application of the STM to NEAs, which are relatively small and often irregularly shaped, may lack the dusty insulating regolith (which reduces the surface thermal inertia) characteristic of larger bodies, and are often observed at large solar phase angles. For these reasons the assumptions inherent in the STM are not generally valid in the case of NEAs. In general, the STM appears to underestimate the diameters and over estimate the albedos of NEAs (Harris and Lagerros, 2002). Lebofsky et al. (1978) proposed an alternative fast-rotating/high-thermal-inertia thermal model that gives results for some NEAs that are in better agreement with diameters and albedos estimated by other means (e.g., from radar observations or spectral class). The Fast Rotating Model (FRM), also called the iso-latitude thermal model, is an alternative model appropriate for use with objects which rotate rapidly or have high surface thermal inertias in which half the thermal emission originates from the night side. The FRM assumes a perfect sphere with its spin axis perpendicular to the plane containing the asteroid, the observer and the Sun, and a temperature distribution depending only on latitude.

Consider an elementary surface strip around the equator of the spherical asteroid. The conservation of energy requires that the solar energy absorbed by the strip on the day side is reemitted as thermal radiation around its entire circumference:

$$\frac{S_0(1-A)}{r^2} 2R^2 d\theta = \varepsilon\sigma T^4 \left(2\pi R^2 d\theta\right) \tag{2-22}$$

where R is the radius of the asteroid and dθ the width of the strip. Eq (2-22) yields the following expression for the sub-solar maximum temperature:

$$T_{SS} = \left[\frac{S_0}{r^2}\frac{(1-A)}{\pi\varepsilon\sigma}\right]^{1/4} \tag{2-23}$$

which is the analogue of Eq (2-16) with η replaced by π. Finally the temperature on the surface of the asteroid is a function of the latitude θ only, i.e.:

$$T(\theta) = T_{SS}\cos^{\frac{1}{4}}\theta \tag{2-24}$$

We have adopted the following algorithm to implement the FRM in this work:

1) Guess the geometric visible albedo p_V.
2) Given the H value, calculate D from Eq. (2-16)
3) From Eq. 2-8 obtain A and calculate T_{SS} using Eq (2-23).
4) Calculate the temperature distribution on the sphere using Eq (2-24)
5) Calculate the model flux

$$F(\lambda_i) = \frac{\varepsilon D^2}{\pi \Delta^2} \int_0^{\pi/2} B(\lambda_i, T(\theta)) \cos^2 \theta d\theta \qquad (2\text{-}25)$$

6) where θ is the latitude in a astro-centric reference frame with the pole orthogonal to the plane containing the Earth and the Sun.
7) Calculate the χ^2

$$\chi^2 = \sum_{i=1}^{N} \left(\frac{(F(\lambda_i) - f(\lambda_i))^2}{\sigma_i^2} \right) \qquad (2\text{-}26)$$

8) Change the value of the p_V parameter and reiterate the algorithm (jumping back to point 2) until the minimum value of the χ^2 is reached.

The value of the p_V at χ^2 minimum is the least-square best estimate for the albedo. Note that the FRM does not require any correction to the thermal flux for the phase angle.

2.7.3 The near-Earth asteroid thermal model (NEATM)

In general, neither the STM nor the FRM provide good fits to the measured spectral energy distributions of NEAs. Harris (1998) showed that it was possible to obtain a good fit to multi-wavelength thermal infrared data of NEAs with a modification to the STM. The NEATM (see Harris, 1998 for further details) assumes the asteroid to have a spherical shape and its surface temperature distribution to be described by Eq (2-18). However, in this model, Eq (2-17), which defines the sub-solar temperature, is used with the difference that the value of η is not set equal to 0.756 as it is in the case of the STM. Within the NEATM, η is a free parameter, which is iteratively adjusted to provide the best fit to the observed thermal infrared fluxes. The effect of changing η is that of changing the object's sub-solar temperature T_{SS} and, as a consequence, the whole surface temperature distribution is scaled by a factor $\eta^{-1/4}$. Moreover, with respect to the STM, the NEATM differs in the way the phase angle is taken into account. Instead of scaling the infrared flux by a factor of 0.01 magnitudes per degree, the phase angle is taken into account by calculating numerically the actual thermal flux an observer would detect from the illuminated portion of a smooth sphere visible to him at a given solar phase angle,

assuming no emission originates on the night side: see Eq (2-28). This treatment assumes a Lambertian emission model and has been applied and discussed by previous authors (e.g., Cruikshank and Jones 1977, Brown 1985). of the STM. The empirical phase coefficient (of 0.01 mag/deg) used with the STM has been derived and tested for solar phase angles no greater than 30°. NEAs, however, are often observed at much higher phase angles (up to 90°) and they surface characteristics (macroscopic roughness, thermal inertia) may differ significantly from those of large main belt asteroids on which the STM was calibrated.

It is important to emphasize that the NEATM requires good wavelength sampling of the thermal continuum (i.e., four or five filter measurements over the range 5 to 20 μm) for a stable fit of the η-parameter to be achieved. If only one or two filter measurements closely spaced in wavelength are available, the derivation of η via spectral fitting is not possible. In such cases a default value of η can be used. Harris (1998) has proposed the value of 1.2 by the comparison of albedos and diameters of objects for which independent information on these parameters is available. Delbò et al. (2003) have first studied the dependence of η values derived by the use of NEATM with the phase angle, α. They suggested that $\eta=1$ for $\alpha<45°$ and $\eta=1.5$ for $\alpha>45°$ provide a best fit to the observed distribution of η values.

The algorithm which implements the NEATM in this work can be described as follows:

1. Guess the geometric visible albedo pV.
2. Given the H value, calculate D from Eq. 2-15
3. From Eq. (2-8) obtain A. Provide an initial guess for the η-value (e.g. $\eta=1$) and calculate TSS using Eq (2-18) and the surface temperature distribution using Eq (2-27)

$$T(\theta,\varphi)=T_{SS}\cos^{1/4}\theta\cos^{1/4}\varphi \qquad (2\text{-}27)$$

for θ in the range $[-\pi/2, \pi/2]$.

4. Calculate the model flux by integrating the Planck's function over the illuminated portion of a smooth sphere visible to the observer

$$F(\lambda_i)=\frac{\varepsilon D^2}{\Delta^2}\int_0^{\pi/2}\int_{-\pi/2}^{\pi/2}B(\lambda_i,T(\theta,\varphi))\cos^2\varphi\cos(\theta-\alpha)d\theta\,d\varphi \qquad (2\text{-}28)$$

where ξ is the angular distance from the sub-solar point (i.e. the colatitude in a reference frame where the pole points toward the Sun).

5. Calculate χ2

$$\chi^2 = \sum_{i=1}^{N}\left(\frac{(F(\lambda_i) - f(\lambda_i))^2}{\sigma_i^2}\right) \tag{2-29}$$

6. Change the value of pV and of the η parameter and reiterate the algorithm (going back to point 2) until the minimum value of the χ2 is reached.

In this work, we have implemented the *Levenberg-Marquardt Method*. (Press et al. 2002) to find the minimum of the χ^2 function of Eq. 2-29.

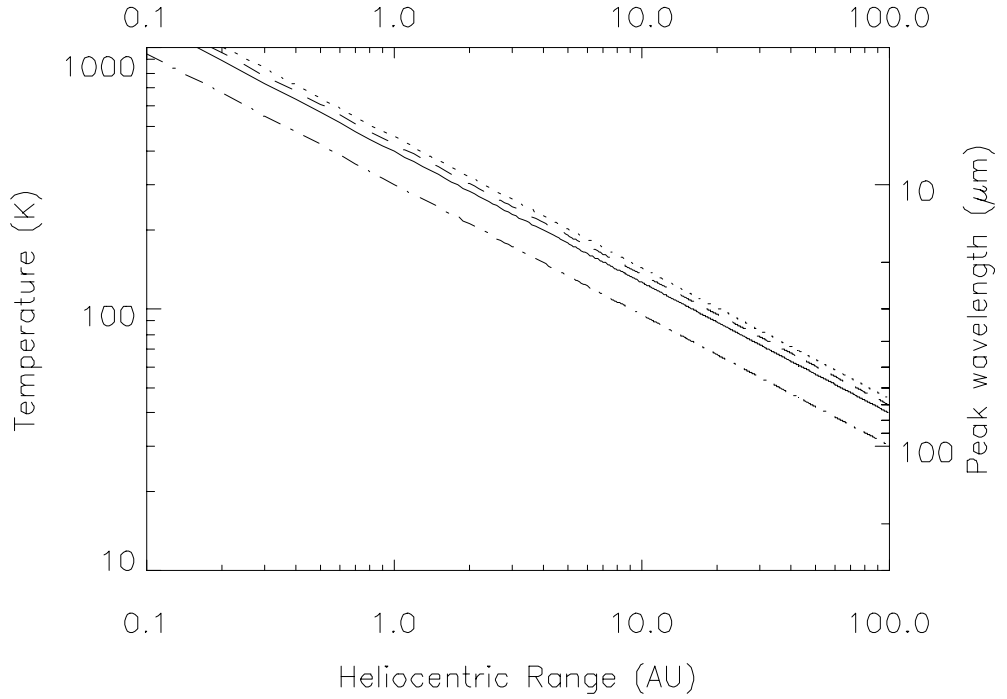

Fig. 2.6 As of Fig. 2.3, but T_{SS} is calculated for different value of the parameter η. Solid-line: η=1.0; dashed-line: η=0.756 as in the "refined" STM of Lebofsky and Spencer (1989); dotted-line: η=0.6, dashed- and dotted-line: η=π which is the value used within the FRM.

It is of interest to point out that the value of T_{SS} in the thermal models we have here described is never equal to the equilibrium value, that Eq (2-8) would give, unless η is derived (in the case of the NEATM) or assumed (as in the case of the STM) equal to one. Fig. 2.6, which is the analogue of Fig. 2.3 for η≠1, shows the dependence of T_{SS} as a function of the heliocentric distance for different values of η and different thermal models.

2.8 Uncertainties

2.8.1 Rotational variability effects and lightcurve correction of infrared fluxes

The thermal infrared flux that an observer receives from an asteroid varies as the object rotates. If fluxes at different wavelengths are measured at different times, as in the case of spectro-photometry obtained with narrow band infrared filters, severe alterations of the shape and of the absolute level of the measured spectral energy distribution may result[6]. Thermal model fits may in those cases give erroneous results. Thermal infrared fluxes can be corrected for rotational variability if visible lightcurve data are available for the time of the thermal observations. Correction of the flux values to the mean lightcurve magnitude is performed on the assumption that the thermal infrared and the visible band lightcurve are identical. Clearly difference in the lightcurve (i.e. in the amplitude, phase and structures) cannot be ruled out and such differences may contribute to the scatter of the data point with respect to the thermal infrared continuum. In those cases in which no lightcurve data are available the uncertainties in the results are inevitably larger and very difficult to be estimated.

2.8.2 The actual temperature distribution differs from the modeled one

Due to their non-zero thermal inertia, real asteroid surfaces are not in instantaneous thermal equilibrium with insolation. Moreover, temperature distributions differing significantly from the Lambertian temperature distribution cannot be ruled out. Several factors influence the actual temperature distribution on the surface of a real body. It is very well known, for instance, that the sub-solar brightness temperature of the Moon seen at zero phase angle is higher than the temperature predicted by the equilibrium with solar radiation (e.g. Sinton, 1962). Furthermore, the temperatures along the equator at full moon vary as $\cos^{1/6}\Omega$ and not as $\cos^{1/4}\Omega$ expected from a Lambertian surface. Statistical studies showed that the falloff in brightness temperature towards the Moon's limb can be represented by a relation linear in $\cos\Omega$ ($T(\Omega)=324.2 +72.6 \cos\Omega$: Shorthill, 1972). The departures of the brightness temperature on the lunar surface can be explained by the effects of surface roughness.

Most asteroids are covered by a very porous soil, similar to the lunar regolith (Housen et al., 1979; McKay et al., 1989). Heat conduction in the regolith is extremely low, because of the high porosity. However, conduction within the porous material plays an important role in determining the surface temperature distribution especially for fast rotating asteroids. Consider a surface element of a body with

[6] On the basis of the experience, rule-of-thumb, practical times required to obtain a measurement in one filter, taking into account overheads, are between 10 and 40 minutes. Considering that typical rotational periods for NEAs are of the order of some hours, it is clear that light curve effects have to be taken into account.

a high thermal inertia: this element behaves like a capacitor or sink for the solar energy, and thus its temperature is not only a function of albedo and heliocentric distance but depends also on its previous thermal history. With the Sun in the equatorial plane, the higher the thermal inertia is the smoother the temperature distribution with respect to longitude is. For a very high thermal inertia and rotation rate the surface element has no time to cool down on the night side: its temperature remains constant through day and night (i.e., it is independent of longitude). The effect of thermal inertia is coupled to rotation rate. A slow rotating asteroid with high thermal inertia displays a similar temperature distribution of one rotating very rapidly but with a lower thermal inertia. It is interesting to anticipate here a result described in Chapter 6. There, we will show calculated diurnal temperature profiles for an asteroid in the near Earth space for different value of the thermal inertia. For relatively low values of this parameter small variation in the range 10-20 K are expected at the sub-solar point, although the night-time temperature can rise up to 200 K. Systematic errors on the resulting diameter and albedo are likely to occur if observations are carried out at large solar phase angle and the thermal emission from the night side is ignored.

2.8.3 Accuracy of the H values

The accuracy of albedo values derived via thermal models depends strongly on the accuracy of the adopted absolute magnitude, H. In those cases in which reliable H-values are not available from other sources, we have resorted to estimates based on the values given by the JPL Horizons (ssd.jpl.nasa.gov/horizons.html), MPC (cfa-www.harvard. edu/iau/MPEph/MPEph.html), and NeoDys (newton.dm.unipi.it/neodys) web sites. It should be noted that the uncertainty in these estimates is often large, e.g., ≥ 0.5 mag. In the event that more reliable H-values become available in the future, the derived albedo and diameter values given in Chapter 3 can be updated using the convenient expressions given by Harris and Harris (1997).

2.9 Thermophysical models

It is clear that the STM and its derivatives are based on assumptions which make simplifications to the physical processes active at the surface of asteroids. Simple models have obvious limitation when a detailed investigation of the physical processes is required from high-quality observational data. The main goal of the work on thermophysical models of asteroids has been to introduce a more detailed description of the physics which governs thermal effect acting on asteroid surfaces, as compared to simple thermal models. Several authors have worked on this topic. For example, Brown (1985) introduced ellipsoids to describe the shapes of asteroids. Spencer (1990) introduced heat conduction in

combination with surface roughness. Lagerros (1996, 1997, 1998, and references therein) collected, combined, and extended these and other approaches into a single working model.

Clearly, thermophysical models are to be preferred over the simple models for accurate results. However, in the case of NEAs, parameters which are required by more complex models, such as shape, thermal inertia, pole orientation, and surface roughness, are normally not known. So, while complex models, such as those described by Lagerros, are important for furthering our understanding of the asteroid thermal processes, their use has severe limitations to derive sizes and albedos of NEAs for which a limited number of radiometric data are available.

2.10 Summary

Observations in the thermal infrared enable albedos and diameters to be derived and give some insight into the thermal properties of an object.

Thermal infrared radiation carries direct information on the size of the object. However, with limited sampling of the spectral energy distribution and with the typical measurement accuracy achieved in the medium infrared from the ground, an unconstrained solution to the problem of Eq 2-3 is unstable. Thermal models are thus required to derive diameters and albedos from radiometric measurements.

The STM was shown to provide reliable diameters and albedos for most large main belt asteroids. However, its use in the case of NEAs gives albedos that are generally too high compared to the results expected from their taxonomic classification.

The failure of the STM to derive reliable albedos for NEAs is very likely due to the different thermal properties of these objects when compared to large MBAs. With their small force of gravity and their very irregular surfaces, NEAs cannot retain a thick layer of insulating regolith and should have more exposed rock than what main belt asteroids have. This results in larger thermal inertias and consequently the hypothesis of instantaneous thermal equilibrium with sunlight at all points on their surface to break down.

The FRM was introduced to derive diameters and albedos of objects which rotate rapidly and/or have high thermal inertia. STM and FRM usually give very different results and choice of which model to use for a particular NEA, in the absence of additional information, is often quite arbitrary.

Harris (1998) have shown that neither the STM nor the FRM provide good fits to the measured spectral energy distribution of the thermal emission of NEAs. However, the fit is considerably improved if the NEATM (a modified STM) is used with a beaming parameter $\eta \geq 1$. The larger beaming

parameters, compared with the value of 0.756 used in the IRAS STM for main-belt asteroids, are consistent with the results of previous authors suggesting that NEAs have larger surface thermal inertias in general than main-belt asteroids.

Moreover, the use of the NEATM allows a first-order correction for the effects of rotation, surface roughness and thermal inertia by fitting the beaming parameter η to the multi-wavelength data to match the observed color temperature.

Application of all three thermal models gives some idea of the modeling uncertainties involved in the measurement of NEA diameters and albedos.